

FIRESIDE CORROSION AND CARBURIZATION OF SUPERHEATER MATERIALS IN SIMULATED OXYFUEL COMBUSTION CONDITIONS

Satu Tuurna, Pekka Pohjanne, Sanni Yli-Olli
VTT Technical Research Centre of Finland, Espoo, Finland

Edgardo Coda, Kyösti Vänskä
Foster Wheeler Energy Ltd, Varkaus, Finland

ABSTRACT

Oxyfuel combustion is considered as one of the most promising technologies to facilitate CO₂ capture from flue gases. In oxyfuel combustion, the fuel is burned in a mixture of oxygen and recirculated flue gas. Flue gas recirculation increases the levels of fireside CO₂, SO₂, Cl and moisture, and thus promotes fouling and corrosion. In this paper the corrosion performance of two superheater austenitic stainless steels (UNS S34710 and S31035) and one Ni base alloy (UNS N06617) has been determined in laboratory tests under simulated oxyfuel conditions with and without a synthetic carbonate based deposits (CaCO₃ - 15 wt% CaSO₄, CaCO₃ - 14wt% CaSO₄ - 1 KCl) at 650 and 720°C up to 1000 hours. No carburization of the metal substrate was observed after exposure to simulated oxyfuel gas atmospheres without deposit, although some carbon enrichment was detected near the oxide metal interface. At 720°C a very thin oxide formed on all alloy surfaces while the weight changes were negative. This negative weight change observed is due to chromium evaporation in the moist testing condition. At the presence of deposits, corrosion accelerated and considerable metal loss of austenitic alloys was observed at 720°C. In addition, clear carburization of austenitic steel UNS S34710 occurred.

Keywords: oxyfuel combustion, corrosion, carburization, high temperature

INTRODUCTION

Fossil fuels are expected to remain the leading fuel sources in power generation for the foreseeable future. The CO₂ emission will have a social and economical impact in energy generation. Carbon dioxide capture and storage (CCS) is considering as a feasible technology for reducing CO₂ emissions while satisfying the ever-growing energy demands [1]. The most cost-effective and readily available option is to mitigate CO₂ emission by increasing the plant efficiency. At the same time new technologies to CO₂ emissions reduction and CCS processes are been developed. In these processes, CO₂ is captured from the cleaned products of combustion or gasification. It has been estimated that CCS for base load power generation is likely to become commercially available at around 2025. The oxyfuel combustion represents a favorable CCS method among wide variety of potential CO₂ capture technologies. Oxyfuel combustion is a process where fuel (fossil fuels or even co-firing of coal and biomass) is burnt using pure oxygen instead of air as the primary oxidant. Since the nitrogen component of air is not heated, fuel consumption is reduced, and higher flame temperatures are possible [2,3]. Compared to conventional air-fired combustion, the oxyfuel process will use a combination of oxygen, with a

purity of more than 95 vol %, and recycled flue gas to combust the fuel. Flue gas recirculation is used to balance combustion and control combustion temperature [2,4]. Produced flue gas consists mainly of CO₂ and water vapour, which is after purification and compression ready for storage. Other major gas components in flue gases are carbon monoxide, nitrogen from fuel and air leakages, and possible enrichments of sulfur oxides and chlorine species due to flue gas recirculation. Experiments in oxyfuel pilot plants have indicated that sulfur concentration can be higher compared to air combustion [5]. The changes in the combustion gas chemistry will also affect the chemistry and formation of deposits, with potentially increasing corrosion and internal attack of the boiler components that are in contact with the combustion and flue gas environment [6-8].

The corrosion mechanisms and life limiting factors in air-fired combustion have been extensively studied over the past years. However, there is still relatively little experimental information available about the effects of oxyfuel combustion on the boiler material performance. The experiments of demonstration scale are on-going with current high temperature materials. Typically the presence of sulfur strongly increases the corrosion rate, but the influence of sulfur on corrosion can be complicated, as in the form of SO₂ it can also slow down corrosion. The phenomenon is dependent on time, fireside environment, gas partial pressures and alloying elements of the tube material [9-11]. In oxyfuel combustion the likelihood of the presence of sticky deposits is increased [12,13]. Sulfation and carbonation of ash particles under oxyfuel combustion is higher due to high SO₂ and CO₂ potential. There are indications that oxide scales developing in O₂/CO₂/H₂O atmospheres are not protective and internal carburization may occur [10,14,15].

Limestone (CaCO₃) is used in oxyfuel circulating fluidized bed (CFB) boilers as absorbent for capture of SO₂. In oxyfuel combustion the CaO - CaCO₃ equilibrium comes close to the normal operating temperature and the capture mechanisms may change from normal sulfation (CaCO₃ - CaO - CaSO₄) to direct sulfation path (CaCO₃ - CaSO₄) due to high CO₂ concentration. In certain components hard deposits may form during the simultaneous occurrence of calcination, sulfation and recarbonation. Such a deposit may cause operational problems like plugging of gas channels and/or corrosion of heat exchanger surfaces. The effects of corrosion and microstructural changes, like carburization, may reduce mechanical properties such as creep and/or fatigue strength and ductility, and thus the expected component life. Austenitic stainless steels are widely used for high temperature applications such as nuclear power plants, boilers, superheaters and chemical reactors. Ni based alloys can withstand harsh environments and exhibit high heat resistance, and thus are in future used at least in some extent in certain energy generation components. Previous studies have shown that the carburization of low alloyed base materials occurs when CaCO₃-based deposits are used, e.g. [16]. The results presented here are a part of the study aiming to experimentally clarify the corrosion resistance of some austenitic and Ni base alloys in simulated oxyfuel combustion conditions.

EXPERIMENTAL

Two superheater austenitic stainless steels (UNS S34710 and S31035) and one nickel base alloy (UNS N06617) have been studied in laboratory tests under simulated oxyfuel conditions with and without synthetic deposits up to 1000 hours, Table 1. Table 2 shows the chemical composition of used materials. Rectangle shape specimens with dimensions of 15 x 15 x 2.5 mm were machined from thick walled tubes. The samples were bright polished with SiC paper (P1200), washed with deionized water and ultrasonically degreased in ethanol. Exposure testing was carried out in horizontal Al₂O₃ tube furnace. The test environments were prepared from premixed and/or pure

gases that were mixed based on flow rates and controlled using calibrated mass-flow controllers. The flow rate of gases was 10 l/h. The carrier gas was passed through a humidifying unit containing deionized water before the furnace, to add moisture to the gas mixture. In tests with synthetic deposit, deposit covered the half of sample.

Table 1: Test matrix

Gas composition	T [°C]	Used deposit	Material
2%O ₂ -29%H ₂ O-44%CO ₂ -0.6%SO ₂ -0.2HCl-N ₂	650	-	S34710, S31035, N06617
		CaCO ₃ - 15 CaSO ₄ wt%	S34710, S31035, N06617
		CaCO ₃ - 14 wt% CaSO ₄ -1 KCl	S34710, S31035
	720	-	S34710, S31035, N06617
		CaCO ₃ - 15 CaSO ₄ wt%	S34710, S31035
		CaCO ₃ - 14 wt% CaSO ₄ -1 KCl	S34710, S31035, N06617

Table 2: Chemical composition of test materials [wt%]

Alloy	Cr	Ni	Mo	Nb	Fe	Other
S34710	18.3	11.7	0.23	0.92	bal.	1.64 Mn, 0.33 Cu, 0.4 Si, 0.07 C
S31035	22.3	24.9		0.5	bal.	3.4 W, 1.5 Co, 2.9 Cu, 0.2 Si, 0.3 Mn, 0.24 N, 0.06C
N06617	23	bal.	9.2	-	1	12.7 Co, 1.2 Al, 0.4 Ti

After testing the samples were moulded in plastic after which the prepared and polished sample cross-sections were analysed using optical and SEM/EDX microscopy to determine the oxide layer thickness and metal loss as well as the elemental distribution in the oxides. The carburization tendency was evaluated from etched cross sections using optical microscopy. Corrosion behaviour of the materials was based on the estimation of the metal loss and depth of internal material degradation. In addition to sample thickness loss, weight change measurements were carried out for the specimens exposed without deposit.

RESULTS AND DISCUSSION

Table 3 summarises the mean values of sample thickness loss and depth of internal degradation below formed oxide scale after 1000 h of exposure at 650 and 720°C under 2%O₂-29%H₂O-44%CO₂-0.6%SO₂-0.2HCl-N₂ gas with and without deposits. After 1000 h exposure at 650°C without deposit UNS S34710 showed more extensive oxidation than S31035. Uneven oxides with a two layer nodule structure formed on the S34710 surface although locally a continuous scale was found in some parts of the sample, Figure 1. Nodule formation has probably started at weak points such as grain boundaries. This nodular growth would have continued until the nodules grow together to form a continuous oxide covering the whole surface. With short exposure times (168 and 500 h), only a very thin oxide film was observed on alloy S34710 surface. EDX analyses showed an iron rich outer oxide layer and a mixed oxide inner layer mainly containing iron, chromium and nickel. Measured weight change was positive, Figure 2. The oxidation rate of UNS S31035 and N06617 alloys was almost negligible at 650°C and only a very thin continuous Cr₂O₃ film formed on the alloy surfaces. At 720°C a thin oxide (~1 µm) formed on all alloy surfaces, Figure 1, and the weight changes were negative. This negative weight change observed is due to chromium evaporation in moist exposure conditions; no spallation of formed scales was seen. It has been shown, e.g. in [17], that under the moist test conditions evaporating metal hydroxides are

formed and thus the protective oxide scale formation is retarded or prevented. The scatter in results at 720°C (no linear weight loss) is probably due to the depletion of surface chromium causing, at least temporary, diminishing of evaporation until new chromium is diffused to the surface area. Figure 2 summarizes the weight change results of the exposures without deposit at 650 and 720°C.

Table 3: Mean thickness loss of sample and depth of internal degradation area below oxide scale after 1000 h exposure at 650 and 720°C under simulated oxyfuel atmosphere with and without deposits. *Internal degradation mostly through grain boundaries

Material	Environment	650°C		720°C	
		Thickness loss	Internal*	Thickness loss	Internal*
S34710	Gas exposure	30 µm	none	<1 µm	none
	with CaCO ₃ – 15 wt% CaSO ₄	300 µm	~50 µm	950 µm	~150 µm
	with CaCO ₃ – 14 CaSO ₄ – 1 wt% KCl	200 µm	~30 µm	400 µm	~150 µm
S31035	Gas exposure	0.5...1 µm	none	<1 µm	none
	with CaCO ₃ – 15 wt% CaSO ₄	400 µm	~50 µm	almost totally destroyed	
	with CaCO ₃ – 14 CaSO ₄ – 1 wt% KCl	300 µm	~80 µm	650 µm	~150 µm
N06617	Gas exposure	<0.5 µm	none	<1 µm	none
	with CaCO ₃ – 14 CaSO ₄ – 1 wt% KCl	-	-	25	~20 µm

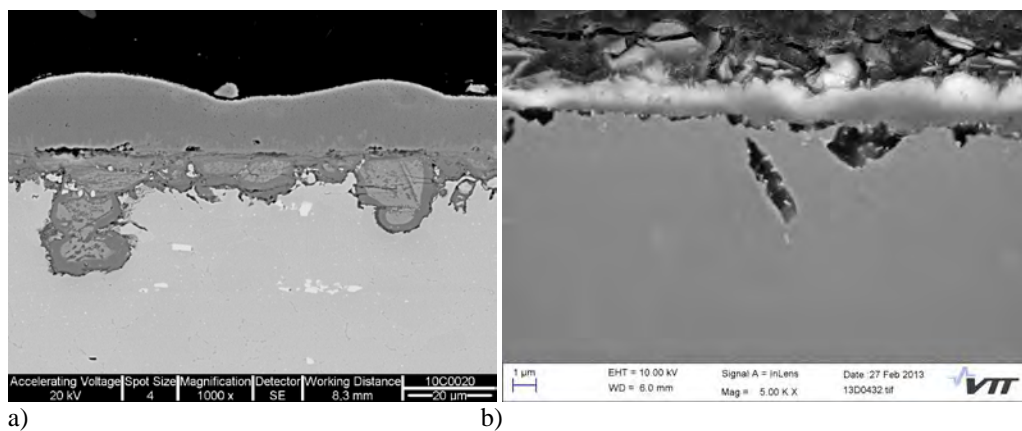
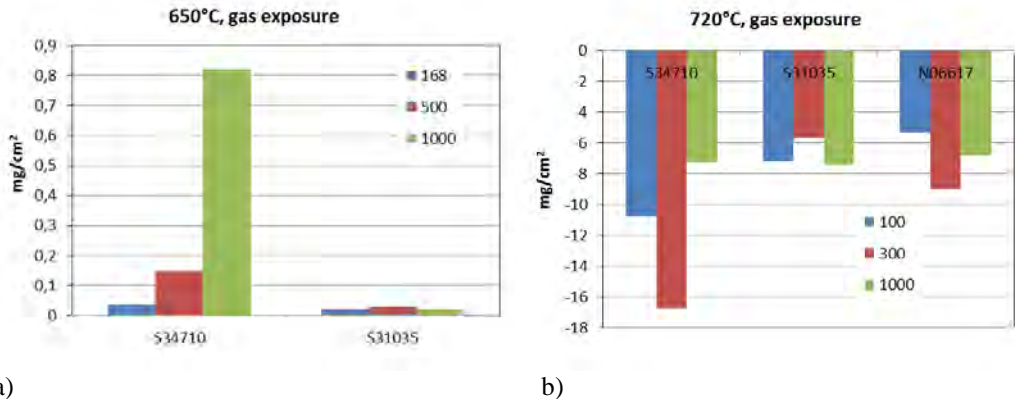


Figure 1: Example of oxides formed on UNS S34710 after 1000 h exposure in atmosphere simulating oxyfuel combustions; Oxide growth at a) 650°C and b) 720°C



a) b)
 Figure 2: Weight change of UNS S34710, S31035 and N06617 after gas exposure testing at a) 650°C and b) 720°C without deposit

Corrosion was visible under deposits on both austenitic stainless steels at 650 and 720°C. At 720°C corrosion of Ni base alloy was also observed. More severe corrosion of austenitic steels was observed with CaCO₃ - 15 wt% CaSO₄ deposit than with CaCO₃ - 14 CaSO₄ - 1 wt% KCl deposit. In the case Ni alloy this could not be seen because Ni alloy was exposed only with KCl containing deposit at 720°C.

The oxide scale on UNS S34710 surface was continuous around the sample both under deposit layer and above it (deposit covered only the half of the sample). Under the deposit layer the formed oxide was some what thicker, and thus the loss of metal was higher. At 650°C a two layer oxide scale was observed. At 720°C the oxide growth accelerated significantly and the outer layer of the oxide was detached. Also the depth of the internal degradation area with chromium depletion increased with increasing temperature. Figure 3 shows the EDX analyses of oxide formed on S34710 surface with CaCO₃ - 15 wt% CaSO₄ deposit. Sulphur was detected inside the oxide scale, and also at grain boundaries under the oxide. No chlorine was observed in the corrosion products with the chlorine containing deposit. This is probably due to sample preparation. In addition to oxidation, carburization by formation of grain boundary carbides in S34710 steel was observed at both exposure temperatures with the both deposits, Figure 4. Surface layer of whole sample was carburized; carburization occurred both in the gaseous environment (in the part of sample above the deposit) and under the deposit. Carbonate based deposits and different corrosion reactions on alloy surface have an effect on carburization due to change of local CO₂ pressure and carbon activity at deposit alloy interface [5]. Corrosion reactions occurring at material surface may change the nature of oxide scale from protective to non-protective allowing carbon and other harmful species to penetrate inside the material. The results from the exposure with CaSO₄ - KCl deposit in simulated oxyfuel conditions did not show carburization of S34710 steel [18]. Figure 5 presents the carbon content of S34710 surface at different depths, determined with optical emission spectrometry (Leco TC-136). The depth of carburization after 1000 h based on Leco measurement and metallography was from 200 up to 400 µm depending on exposure temperature.

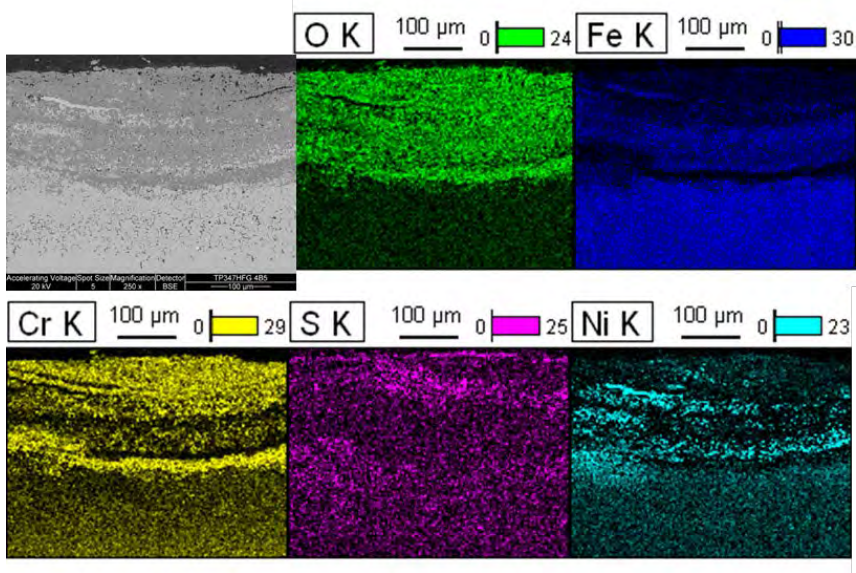
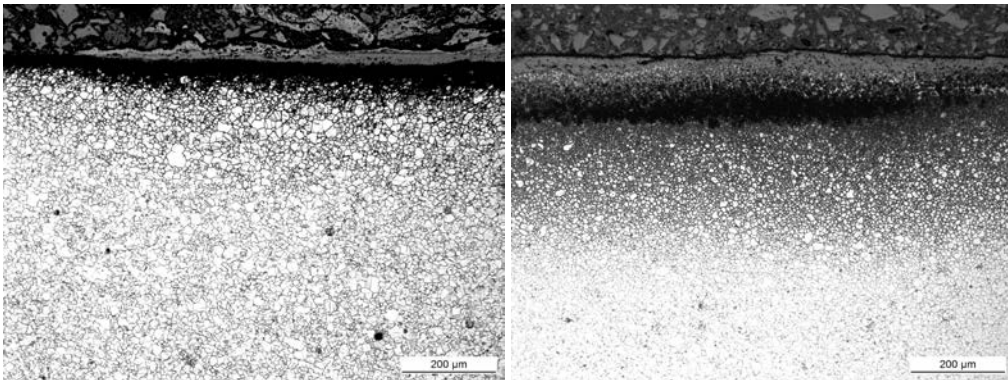


Figure 3: EDX analyses of oxide formed on S34710 steel after 1000 h exposure at 720°C with $\text{CaCO}_3 - 15 \text{ wt}\% \text{CaSO}_4$ deposit



a) b)
Figure 4: Carburization of S34710 after 1000 h under $\text{CaCO}_3-15 \text{ wt}\% \text{CaSO}_4$ deposit with simulated oxyfuel conditions at a) 650°C and b) 720°C

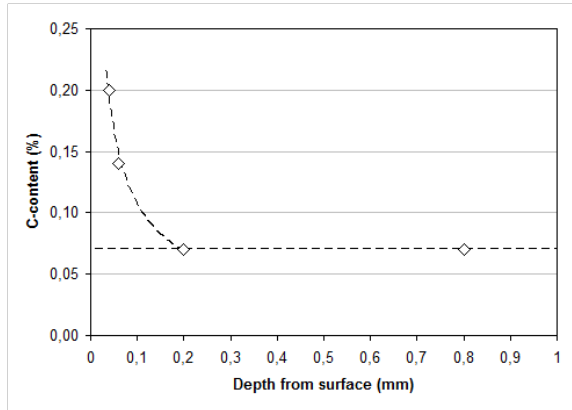


Figure 5: Carbon content on S34710 under CaCO_3 -15 wt% CaSO_4 deposit after exposure in simulated oxyfuel conditions for 1000 h at 650°C

The part of UNS S31035 samples covered with deposit suffered from accelerated corrosion. Whereas only a thin oxide layer and some deeper pits through grain boundaries were detected in the part of samples exposed to gaseous environment (above the deposit), Figure 6. It seems that the deposit cannot destroy the formed Cr_2O_3 film on the upper part of the samples, at least during 1000 h exposure testing. Figures 7 and 8 presents EDX analyses of S31035 alloy exposed to CaCO_3 - 15 wt% CaSO_4 and CaCO_3 - 14 wt% CaSO_4 - KCl deposits. The temperature increase accelerated corrosion, especially with CaCO_3 - 15 wt% CaSO_4 deposit, and the part of sample covered with deposit was almost completely destroyed. Sulphur was detected in the oxide structures and the internal degradation area below oxide scale. No carburization of S31035 steel was detected by optical microscopy.

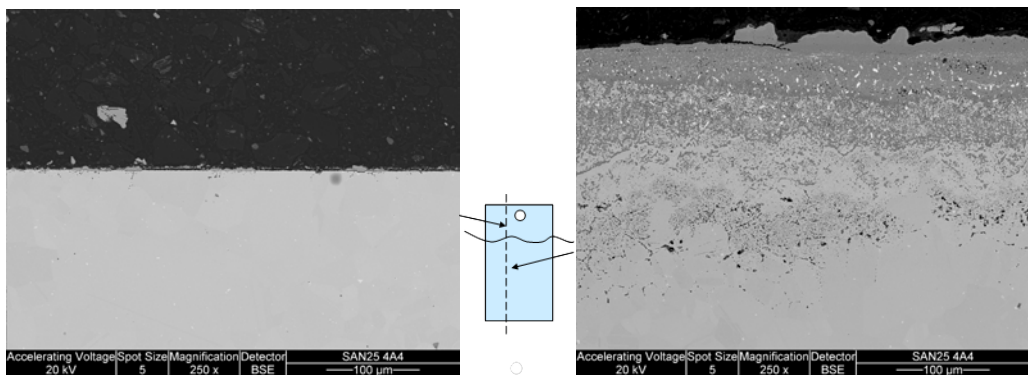


Figure 6: Oxide scale morphology on UNS S31035 after 1000 h exposure with CaCO_3 - CaSO_4 -KCl deposit in oxyfuel conditions at 720°C, under gas phase (left) and under deposit (right). A schematic specimen between micrographs shows sectioning and positions of inspection

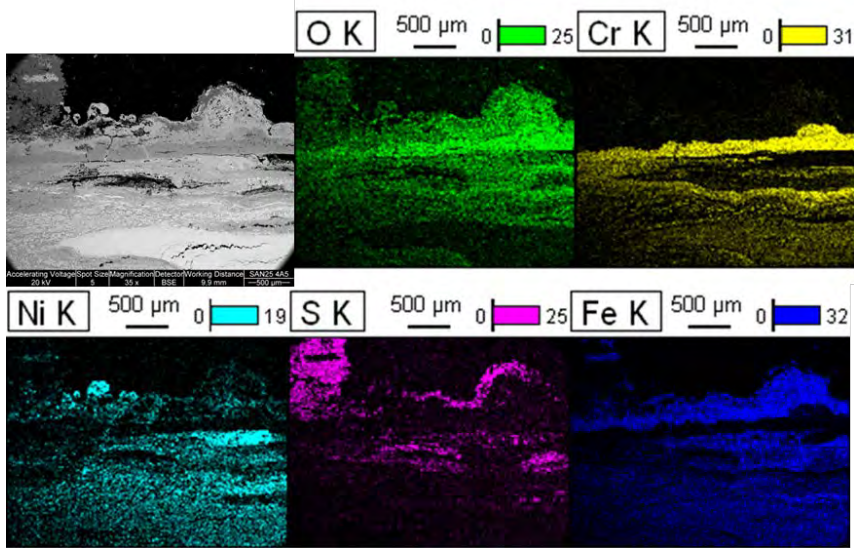


Figure 7: EDX analyses of the oxide scale on S31035 after 1000 h exposure at 720°C with $\text{CaCO}_3\text{-CaSO}_4$ deposit. Sample tip almost totally corroded

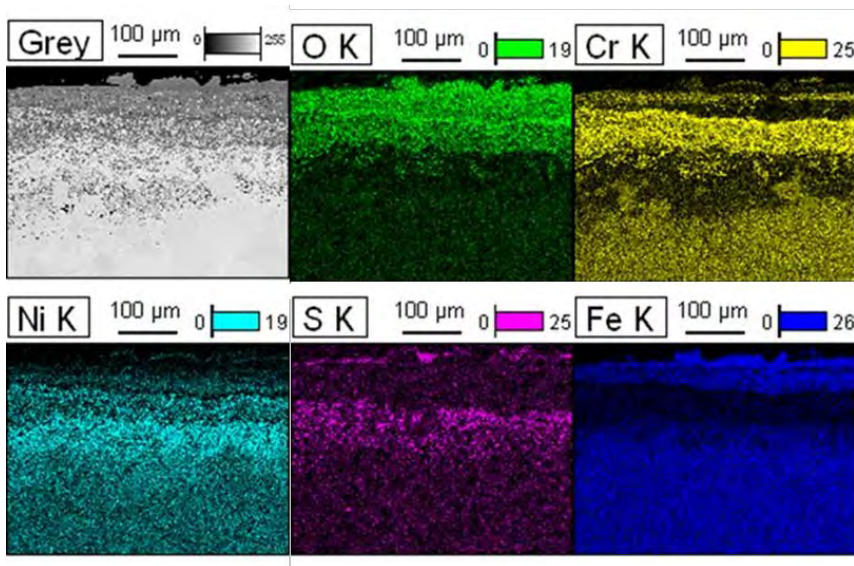


Figure 8: EDX analyses of the oxides on S31035 after 1000 h exposure at 720°C with $\text{CaCO}_3\text{-CaSO}_4\text{-KCl}$ deposit

Figure 9 shows the EDX analyses of N06617 alloy after 1000 h at 720°C with the chlorine containing deposit. Chromium oxide formed on the alloy surface was still thin, however below oxide layer there was the internal degradation area where sulphur was detected. No chlorine was observed.

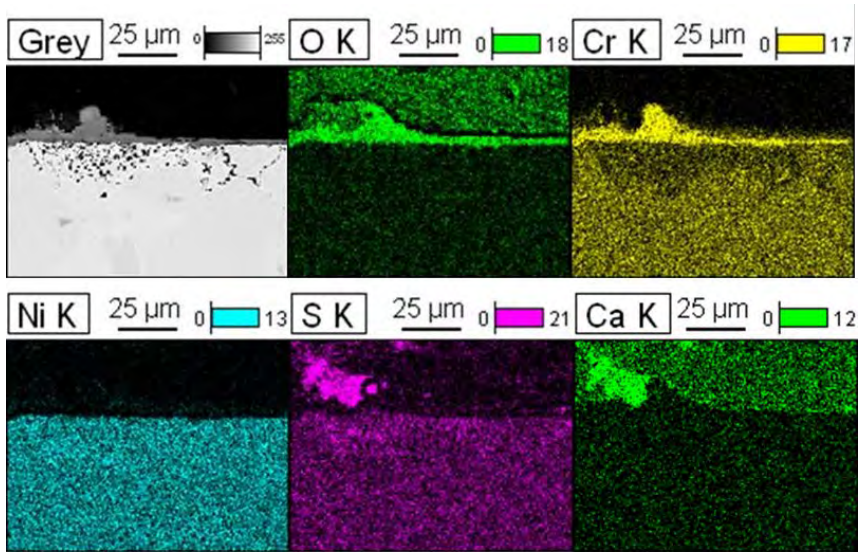


Figure 9: EDX analyses of the oxide on N06617 after 1000 h exposure at 720°C with CaCO_3 - CaSO_4 -KCl deposit

CONCLUSIONS

The results imply that without a deposit, the oxidation rate under simulated oxyfuel conditions (2% O_2 -29% H_2O -44% CO_2 -0.6% SO_2 -0.2% HCl - N_2) is very reasonable at 650°C after 1000 h for the tested materials. At 720°C formed oxide thickness was also quite low, however negative weight change was observed due to chromium evaporation and no spallation of formed scales was seen. Chromium based oxides was observed on material surfaces. No carburization of the metal substrate was observed after exposure to simulated oxyfuel gas atmospheres without deposit, although some carbon enrichment was detected near the oxide metal interface. With extended exposure time, the oxide scale properties may change to enable metal carburization.

With deposits the thicknesses of oxide scales and metal losses of the stainless grades increased with increasing temperature. Some sulphur penetration was observed through grain boundaries in chromium depletion area under oxide scales. At 720°C oxidation rate was higher and the part of the oxide scale, probably outer Fe-rich layer, had peeled off from austenitic stainless steels. UNS S31035 steel corroded most, especially with CaCO_3 - CaSO_4 deposit, and the part of sample covered with deposit was almost completely destroyed. Corrosion of the Ni alloy also increased at 720°C, although the formed oxide after 1000 h was thin, some internal degradation was observed. High Cr or total alloying does not guarantee corrosion resistance in severe conditions. Modification of other properties like grain size may give additional protection against corrosion.

Exposure with the carbonate deposit resulted in corrosion and carburization by formation of grain boundary carbides in the UNS S34710 steel. Earlier results [16] suggested that the critical Cr and Ni content limits for carburization are around 20% under the applied gas and deposit environments. Current results of S31035 grade support this observation. The limits may be affected by the Cr/Ni ratio, extended time of exposure, and changes in the chemical and thermodynamic equilibria of the surfaces due to gradual modification in alloys, its oxides and

deposits. The effects of corrosion and microstructural changes, like carburization, may reduce mechanical performance such as creep and/or fatigue strength and ductility, and thus the expected component life.

ACKNOWLEDGEMENTS

The authors would like to acknowledge the financial support from VTT Technical Research Centre of Finland, Tekes and EU-FP7 Energy MacPlus project (contract 249809). The authors would also like to acknowledge the skilful assistance of T. Kinnunen, J. Veivo, T. Lehtikuusi, J. Metsäjoki and A. Kukkonen.

REFERENCES

- [1] Energy Technology Perspectives 2008 – Scenarios & Strategies to 2050, IEA 2008
- [2] Oxy-fuel combustion for power generation and carbon dioxide capture (Ed. Ligang Zheng) Woodhead Publishing Series in Energy (Cambridge, UK, 2011), pp. 1-9
- [3] Hack, H., Fan, Z., Seltzer, A., "Advanced Oxyfuel Combustion Leading to Zero Emission Power Generation", *Proc 35th International Technical Conference on Clean Coal & Fuel Systems Clearwater*, Clearwater, FL, June, 2010.
- [4] Scheffknecht, G. et al, "Oxy-fuel coal combustion—A review of the current state-of-the-art," *Int. J. of Greenhouse Gas Control*, Vol 5S (2011), pp. 16–35.
- [5] Kranzmann, A. et al, "The challenge in understanding the corrosion mechanisms under oxyfuel combustion conditions," *Int. J. of Greenhouse Gas Control*, Vol 5S (2011), pp. 168–178.
- [6] Hjörnhede, A. et al, "Preliminary Experiences with Materials Testing at the Oxyfuel Pilot Plant at Schwarzepumpe," *Proc. 9th Liege Conference on Materials for Advanced Power Engineering*, Liege, Belgium. 2010 pp. 1220-1235 .
- [7] Wigley, F., Goh, B. "Characterisation of Rig Deposits from Oxy-coal Combustion," *1st Oxyfuel Combustion Conference*, Cottbus, Germany. 2009.
- [8] Stein-Brzozowska et al., "Influence of Oxy-Coal on Fly Ash Transformations and Corrosion Behavior of Heat-Exchangers," *Proc. Oxyfuel Combustion Conference 2*, Queensland, Australia, September. 2011.
- [9] Covino, B., Matthes, S., Bullard, S. "Effect of Oxyfuel Combustion on Superheater Corrosion," *NACE Corrosion 2008*, Houston, Texas, March. 2008. Paper No. 8456.
- [10] Natesan, K., Rink, D.L. "Corrosion Performance of Structural Alloys for Oxy-fuel Combustion Systems," *Proc 21st Fossil Energy Materials Conference*, Knoxville, TN, May. 2007.
- [11] Fryda, L. Sobrino, C., Cieplik, M., van de Kamp, W.L., "Study on Ash Deposition under Oxyfuel Combustion of Coal/Biomass Blends," *Fuel*, Vol. 89, 2010, pp. 1889-1902.
- [12] Stein-Brzozowska, G., Maier, J., Scheffnecht, G. "Deposition Behaviour and Superheater Corrosion under Coal Fired Oxyfuel Conditions," *IEAGHG Special Workshop on SO₂/SO₃/Hg/ Corrosion Issue under Oxyfuel Combustion Conditions*, London, January. 2011.
- [13] Hünert, D., Schulz, W., Kranzmann, A. "Corrosion of Steels in H₂O-CO₂ Atmospheres at Temperatures between 500°C and 700°C," *ICPWS XV*, Berlin, September. 2008.
- [14] Piron Abellan, J., Olszewski, T., Penkalla, H.J., Meier, G.H., Singheiser, L., Quadackers, W.J., "Scale Formation Mechanisms of Martensitic Steels in High CO₂/H₂O-Containing Gases Simulating Oxyfuel Environments," *Mater. High Temp.*, Vol. 26, No. 1 (2009), pp. 63-72.

- [15] Sellakumar, K.M., Conn R., Bland, A. "A Comparison Study of ACFB and PCFB Ash Characteristics," *Proc 6th International Conference on Circulating Fluidized Beds*, Wurzburg, Germany August. 1999.
- [16] Pohjanne, P., Tuurna, S., Auerkari, P. "Fireside Corrosion and Carburization of Superheater Materials in Oxyfuel Combustion," *NACE Corrosion 2012*, Salt Lake City, UT, March. 2012, pp. 4969 – 4980.
- [17] Saunders, S.R.J., Monteiro, M., Rizzo, F., "The oxidation behaviour of metals and alloys at high temperatures in atmospheres containing water vapour: A review," *Prog. Mater. Sci.*, Vol. 53 (2008), pp. 775–837.
- [18] Tuurna, S., Yli-Olli S., Pohjanne, P. "Corrosion and Carburization of Superheater Materials in Oxyfuel Combustion," *Proc. Baltica IX Int. Conference on Life Management and Maintenance for Power Plant Components*, Helsinki-Stockholm-Helsinki, June, 2013, pp. 527-537.